

**A FAMILY OF EQUILIBRIA AND LIMIT CYCLES IN A  
TRI-TROPHIC MODEL WITH TWO DELAYS**AHMAD ALMASRI  AND V.G. TSYBULIN *Communicated by P.P. PETROV*

**Abstract:** We investigate a delayed intraguild predation (IGP), or tri-trophic model that incorporates intraspecific competition and two distinct time delays, capturing gestation and handling effects. The system exhibits rich dynamics, including multistability and delay-induced oscillations. Using analytical techniques, we establish the existence of a continuous family of positive equilibria produced by cosymmetry. We investigate the stability of the equilibria from this family and define delays under which Poincaré–Andronov–Hopf bifurcations occur. The stability of the equilibria in the continuous family depends on the combination of time delays. Numerical simulations confirm the analytical predictions and illustrate how delays selectively destabilize parts of the equilibrium family. These findings highlight the complex interplay between time delays and multistability in shaping the dynamics of tri-trophic ecological systems.

**Keywords:** mathematical ecology, prey–predator–superpredator, differential equations, cosymmetry, multistability, delay.

## 1 Introduction

Intraguild predation (IGP) – a complex ecological interaction involving simultaneous competition and predation among species — plays a significant role in shaping community structure and biodiversity [1, 2]. Mathematical modeling of IGP systems has provided insights into the dynamic behaviors observed in natural ecosystems, including coexistence, extinction, and complex oscillatory patterns [3, 4, 5, 6]. Incorporating delays such as gestation periods, maturation times, and handling times into these models has enriched the understanding of the temporal dynamics and stability properties inherent to ecological interactions [7, 8].

The stability and asymptotic properties of solutions in biological systems with delay were analyzed using theory of functional differential equations [9, 10]. Specific applications to population dynamics, including predator-prey interactions and other living systems models, are investigated to establish conditions for local stability and characterize long-term behavior [11, 12, 13].

Recent studies on three-species prey–predator–superpredator systems have incorporated time delays of distinct biological origin, which can be broadly classified into three types. The first type is the gestation delay, representing the lag between prey consumption and the corresponding growth in predator biomass. This delay has been shown to be the primary driver of stability switches in tri-trophic food chains [14, 15]. The second type is the maturation or stage-structure delay, reflecting the time required for juvenile predators or intraguild prey to reach reproductive maturity [16, 17]. The third type is the handling time delay, associated with the time a superpredator requires to process captured prey, which enters the functional response and governs foraging efficiency. Models incorporating this delay alongside a gestation delay — including two-delay intraguild predation systems — have demonstrated that the two delays interact cooperatively to destabilize equilibria and generate persistent oscillations [18, 19, 20].

Vital problems require a study of the coexistence of species and the possibility of multiple scenarios for population system evolution. Research in physics and biology has yielded important results about multistability and its influence on dynamics and processes [21, 22, 23]. Multistability in predator-prey IGP systems was examined in [6, 24, 25] by using the cosymmetry theory [26, 27, 28]. The continuous family of equilibria for the IGP model was first detected in [6]. The appearance of a family of oscillatory regimes was found and studied in [25]. However, the combined effect of multiple time delays on a system possessing a cosymmetry-induced family of equilibria remains unexplored. This work aims to bridge that gap by investigating how two distinct delays selectively influence the stability landscape of a tri-trophic IGP model with an inherent continuum of steady states.

We consider a delayed prey–predator–superpredator model that accounts for both intra- and interspecies interactions. The prey  $x$  grows logistically and is consumed by two predator populations  $y$  and  $z$ . The predator  $y$  hunts

on  $x$  and is also consumed by the superpredator  $z$ . The system incorporates time delays  $\tau_1$  and  $\tau_2$  to describe gestation or handling times in predator responses. [The inclusion of discrete time delays reflects biologically realistic processes, which introduce memory effects into population growth.](#) The resulting system of delay differential equations is given by:

$$\begin{aligned}\frac{dx}{dt} &= x(1 - x - y - z) \\ \frac{dy}{dt} &= -\mu_1 y + \eta_1 x(t - \tau_1) y(t - \tau_1) - d_1 z y \\ \frac{dz}{dt} &= -\mu_2 z + \eta_2 x(t - \tau_1) z(t - \tau_1) + d_2 y(t - \tau_2) z(t - \tau_2).\end{aligned}\tag{1}$$

The first equation describes logistic growth of the prey population with limitations arising from both self-regulation and predation. The second and third equations model the delayed predator–prey interactions/ The reproduction of  $y$  depends on a time-lagged predation term  $\eta_1 x(t - \tau_1) y(t - \tau_1)$ , while the dynamics of  $z$  involve two delayed interactions—one with the basal resource and another with the intermediate predator—via the terms  $\eta_2 x(t - \tau_1) z(t - \tau_1)$  and  $d_2 y(t - \tau_2) z(t - \tau_2)$ , respectively. Parameters  $\eta_1, \eta_2$  characterize the consumption of prey by predator and superpredator,  $d_1, d_2$  define the consumption of a predator by the superpredator and  $\mu_1, \mu_2$  are the natural mortalities for predator and superpredator.

This paper is organized as follows. We begin by identifying the equilibrium points of system (1) in Section 2. In Section 3, conditions for a nontrivial cosymmetry and parameters leading to the continuous family of equilibria are derived. The stability of these family members is also analyzed. Numerical simulations presented in Section 4 illustrate the dynamic behavior near the continuous family of equilibria. Different delay scenarios are listed, specifically the cases of a single non-zero delay ( $\tau_1 = 0, \tau_2 \neq 0$  and  $\tau_2 = 0, \tau_1 \neq 0$ ) and equal delays ( $\tau_1 = \tau_2$ ). Finally, Section 5 provides a concluding discussion of the results.

## 2 Equilibrium points

System (1) has one trivial equilibrium  $E_0 = (0, 0, 0)$ , one axial equilibrium  $E_1 = (1, 0, 0)$ , irrespective of any parametric restriction, and some boundary equilibria.

The superpredator–absent equilibrium exists and is stable when  $\eta_1 > \mu_1$

$$E_2 = \left( \frac{\mu_1}{\eta_1}, 1 - \frac{\mu_1}{\eta_1}, 0 \right).$$

Predator–absent equilibrium is stable when  $\eta_2 > \mu_2$

$$E_3 = \left( \frac{\mu_2}{\eta_2}, 0, 1 - \frac{\mu_2}{\eta_2} \right).$$

Under some conditions on parameters there exists the interior equilibrium  $E_4 = (x_4, y_4, z_4)$ . It corresponds to the scenario when all three interacting species will survive,

$$\begin{aligned} x_4 &= \frac{1}{a}(-d_1 d_2 + d_1 \mu_2 - d_2 \mu_1), \quad a = -d_1 d_2 + d_1 \eta_2 - d_2 \eta_1, \\ y_4 &= \frac{1}{a}(-d_1 \mu_2 + d_1 \eta_2 + \mu_1 \eta_2 - \mu_2 \eta_1), \\ z_4 &= \frac{-1}{a}(-d_2 \mu_1 + d_2 \eta_1 + \mu_1 \eta_2 - \mu_2 \eta_1). \end{aligned}$$

To analyze the local stability of the equilibria of the delay system, we provide linearization of the system on the steady state  $(x_4, y_4, z_4)$ . Setting the perturbations as  $\mathbf{u} = (u_1, u_2, u_3)$ ,  $x(t) = x_4 + u_1(t)$ ,  $y(t) = y_4 + u_2(t)$ ,  $z(t) = z_4 + u_3(t)$ , the linearized system has the form

$$\frac{d\mathbf{u}}{dt} = J_0 \mathbf{u}(t) + J_{\tau_1} \mathbf{u}(t - \tau_1) + J_{\tau_2} \mathbf{u}(t - \tau_2) \quad (2)$$

where the instantaneous Jacobian matrix  $J_0$  is

$$J_0 = \begin{pmatrix} 1 - 2x_4 - y_4 - z_4 & -x_4 & -x_4 \\ 0 & -\mu_1 - d_1 z_4 & -d_1 y_4 \\ 0 & 0 & -\mu_2 \end{pmatrix} \quad (3)$$

and the delay matrices  $J_{\tau_1}$  and  $J_{\tau_2}$  correspond to terms involving delayed variables:

$$J_{\tau_1} = \begin{pmatrix} 0 & 0 & 0 \\ \eta_1 y_4 & \eta_1 x_4 & 0 \\ \eta_2 z_4 & 0 & \eta_2 x_4 \end{pmatrix}, \quad J_{\tau_2} = \begin{pmatrix} 0 & 0 & 0 \\ 0 & 0 & 0 \\ 0 & d_2 z_4 & d_2 y_4 \end{pmatrix}. \quad (4)$$

The characteristic equation determining stability is given by

$$\det(\sigma I - J_0 - e^{-\sigma \tau_1} J_{\tau_1} - e^{-\sigma \tau_2} J_{\tau_2}) = 0, \quad (5)$$

Here,  $I$  denotes the  $3 \times 3$  identity matrix, and  $\sigma$  is the spectral parameter. The exponential terms  $e^{-\sigma \tau_1}$  and  $e^{-\sigma \tau_2}$  incorporate the effects of time delays in the feedback loops.

At the extinction equilibrium  $E_0$ , the delay-dependent Jacobian matrices  $J_{\tau_1}$  and  $J_{\tau_2}$  are null. The characteristic equation (5) reduces to  $\det(\sigma I - J_0) = 0$ , yielding the eigenvalues directly:

$$\sigma_1 = 1, \quad \sigma_2 = -\mu_1, \quad \sigma_3 = -\mu_2.$$

Since  $\sigma_1 = 1 > 0$ , the equilibrium  $E_0$  is unstable for all parameter values and delays  $\tau_1, \tau_2 \geq 0$ .

**Lemma 1.** *The equilibrium  $E_1$  is locally asymptotically stable for all delays  $\tau_1, \tau_2 > 0$  when  $\mu_1 > \eta_1$ ,  $\mu_2 > \eta_2$ .*

*Proof.* At the predator-free equilibrium  $E_1$ , the Jacobian matrix  $J_{\tau_2}$  is zero. The characteristic equation (5) takes the form:

$$(\sigma + 1)g(\sigma) = 0, \quad g(\sigma) = (\sigma + \mu_1 - \eta_1 e^{-\sigma \tau_1})(\sigma + \mu_2 - \eta_2 e^{-\sigma \tau_1})$$

The first factor gives  $\sigma = -1$ . The stability of  $E_1$  is thus governed by the two transcendental equations associated with the predator ( $y$ ) and superpredator ( $z$ ) populations. Here,  $\mu_1, \mu_2, \eta_1, \eta_2 > 0$  and  $\tau_1 > 0$ . We now analyze the distribution of zeros of  $g(\sigma)$ . When  $\mu_1 > \eta_1, \mu_2 > \eta_2$ . All roots of  $g(\sigma)$  have negative real parts. Specifically, there exists a unique negative real root, and all complex roots satisfy  $\Re(\sigma) < 0$ . Therefore, the equilibrium  $E_1$  is locally asymptotically stable for all delays  $\tau_1, \tau_2 \geq 0$ . Conversely, if  $\mu_1 < \eta_1$  or  $\mu_2 < \eta_2$ . The function  $g(\sigma)$  possesses a positive real root. Consequently,  $E_1$  is unstable.  $\square$

**Remark 1.** *when  $\mu_1 = \eta_1$  ( $\mu_2 = \eta_2$ ), the equilibrium  $E_2$  ( $E_3$ ) branches off from  $E_1$  in a transcritical bifurcation.*

The stability analysis for other equilibria may be done only for specific values of parameters. For example, the case  $\tau_1 = \tau_2$  was considered for the Bazykin model in [29], where no continuous family of equilibria was found. Furthermore, the study in [6], the study with  $\tau_i = 0$  ( $i = 1, 2$ ) revealed multistability, demonstrating that multiple stable states can exist under additional parameter conditions.

### 3 Cosymmetry

V.I. Yudovich [26] introduced the concept of cosymmetry to explain the emergence of a continuous family of equilibria with a varying stability spectrum. In particular, cosymmetry is a vector field orthogonal to the right-hand side of a system of first-order autonomous differential equations. The continuous family of equilibria associated with cosymmetry differs from an orbit under a symmetry group action in that the stability spectrum of the equilibria varies along the family [27]. The family itself may consist of intervals of linearly stable and unstable equilibria. The stability of an equilibrium means its asymptotic stability in the manifold (subspace) transversal to the family.

To find multistability in system (1), we define a vector orthogonal to the right-hand side of the system of differential equations without delays. To obtain such a vector, some additional constraints on the system parameters are required. Then we verify that this vector (cosymmetry) does not vanish at the equilibria  $E_2$  and  $E_3$ . In this case, each given equilibrium belongs to a family [26].

**Proposition 1.** *Under the parameter conditions:*

$$\mu_2 = d_2 \left( 1 + \frac{\mu_1}{d_1} \right), \quad \eta_2 = d_2 \left( 1 + \frac{\eta_1}{d_1} \right). \quad (6)$$

*the system (1) has a cosymmetry*

$$L = \left[ yz, -\frac{1}{d_1}xz, \frac{1}{d_2}xy \right]^T \quad (7)$$

and possesses a continuous family of equilibria given by

$$Q = \left\{ x \in \left[ \frac{\mu_1}{\eta_1}, \frac{d_1 + \mu_1}{d_1 + \eta_1} \right], \quad y = 1 + \frac{\mu_1}{d_1} - \left(1 + \frac{\eta_1}{d_1}\right)x, \quad z = \frac{\eta_1 x - \mu_1}{d_1} \right\} \quad (8)$$

*Proof.* For  $\tau_i = 0$ , multiplying the right side of system (1) on cosymmetry (7), we get:

$$\begin{aligned} \langle F, L \rangle = & xyz \left[ 1 - x - y - z + c_1(-\mu_1 + \eta_1 x - d_1 z) \right. \\ & \left. + c_2(-\mu_2 + \eta_2 x + d_2 y) \right] \end{aligned} \quad (9)$$

After substitution (7) to (9) and simplification, we obtain  $\langle F, L \rangle = 0$ . This means that the vector function  $L$  is orthogonal to the right-hand side of the system (1), i.e.,  $L$  is a cosymmetry of the system.  $\square$

It should be noted that the family of equilibria includes the boundary equilibrium  $E_2$  ( $x = \frac{\mu_1}{\eta_1}$ ) and the equilibrium  $E_3$  ( $x = \frac{d_1 + \mu_1}{d_1 + \eta_1}$ ).

**Proposition 2.** *System (1) under conditions (6) and  $\tau_1 = \tau_2 = 0$  has a continuous family of stable equilibria (8).*

*Proof.* In the absence of delays ( $\tau_1 = \tau_2 = 0$ ) and under conditions (6), the characteristic equation (5) reduces to

$$\det(\sigma I - J_0 - J_{\tau_1} - J_{\tau_2}) = 0, \quad (10)$$

and the stability of the family of equilibria is determined by the eigenvalues of the matrix  $J = J_0 + J_{\tau_1} + J_{\tau_2}$ . The Jacobian matrix at the family of equilibria (8) is given by:

$$J_Q = \begin{bmatrix} -x & -x & -x \\ y\eta_1 & 0 & -yd_1 \\ z\eta_2 & zd_2 & 0 \end{bmatrix} \quad (11)$$

The characteristic equation for  $J_Q$  is written as:

$$\sigma^3 + A_2\sigma^2 + A_1\sigma = 0$$

where

$$\begin{aligned} A_2 &= x \\ A_1 &= \eta_1 xy + \eta_2 xz + d_1 d_2 yz \end{aligned} \quad (12)$$

The zero root  $\sigma_1 = 0$  corresponds to neutral stability along the family  $Q$ . Since  $A_1, A_2 > 0$ , the equilibria of the family  $Q$  are stable.  $\square$

The family of equilibria (8) exists for any values of  $\tau_1$  and  $\tau_2$ . Notably, any point  $x \in \left[ \frac{\mu_1}{\eta_1}, \frac{d_1 + \mu_1}{d_1 + \eta_1} \right]$  constitutes an equilibrium, and it can be realized through the appropriate choice of initial history functions on  $t \in [-\tau_{\max}, 0]$ , where  $\tau_{\max} = \max(\tau_1, \tau_2)$ . For nonzero delays  $\tau_i$  ( $i = 1, 2$ ), the stability analysis of equilibria belonging to the family requires numerical computations. Only a few special cases can be treated analytically.

**Lemma 2.** *For the case  $\tau_1 = 0$ , the boundary equilibria  $E_2$  and  $E_3$  are locally asymptotically stable for any  $\tau_2 > 0$ .*

*Proof.* Under the cosymmetry conditions in (6), the characteristic equation at the boundary equilibrium  $E_2$  (where the superpredator is absent,  $z = 0$ ) is:

$$\sigma + d_2 y (1 - e^{-\sigma \tau_2}) = 0. \quad (13)$$

We first observe that this equation admits no real roots  $\sigma > 0$  or  $\sigma < 0$ . Assume  $\sigma = i\omega$  with  $\omega > 0$ . Separating real and imaginary parts leads to

$$d_2 y (1 - \cos(w\tau_2)) = 0, \quad w + d_2 y \sin(w\tau_2) = 0. \quad (14)$$

Since  $d_2 y > 0$ , the first equality implies  $\cos(w\tau_2) = 1$ , hence  $w\tau_2 = 2\pi k$ ,  $k \in \mathbb{Z}$ . Substituting into the second equation (14) yields  $\omega = 0$ , contradicting  $w > 0$ . Therefore, there exist no nonzero purely imaginary roots  $\sigma = i\omega$  of (13). The only root on the imaginary axis is  $\sigma = 0$ .

At the boundary  $E_3$  (where the predator is absent,  $y = 0$ ), the characteristic equation  $\sigma(\sigma^2 + x\sigma + \eta_2 xz) = 0$ , which is independent of  $\tau_2$ . Consequently, the stability of this boundary equilibrium is unaffected by the delay  $\tau_2$ .  $\square$

Furthermore, we present numerical results for specific parameter values that demonstrate a scenario of partial instability within the family of equilibria.

## 4 Numerical analysis

To investigate the system's dynamics, we use MATLAB with the DDE-BIFTOOL package [30] for numerical continuation and bifurcation analysis. This approach enables a detailed exploration of its response to variations in the delay parameters. The values of the parameters are taken as:  $\mu_1 = 1$ ,  $\eta_1 = 10$ ,  $d_1 = 1$ ,  $d_2 = 1$ , and  $\mu_2, \eta_2$  satisfying (6).

The regime map on the parameter plane  $\eta_2$  and  $\mu_2$  is displayed in Fig. 1. Symbol  $E_j$  marks the stability domain for the equilibrium  $E_j$ ,  $j = 2, 3, 4$ . Stable equilibria  $E_2$  and  $E_3$  coexist for the parameter values within the bistability region  $E_{2,3}$ . The domains  $E_2$ ,  $E_3$ ,  $E_4$ , and  $E_{23}$  share a point  $F$ , which corresponds to the family of equilibria. The symbol  $C$  denotes the region of values for which limit cycles exist for  $\tau_1 = \tau_2 = 0$ . Fig. 1 also shows the region  $C_\tau$  obtained through a computational experiment for  $\tau_1 = \tau_2 = 0.05$ . This region  $C_\tau$  represents the parameters  $(\eta_2, \mu_2)$  for which the equilibrium  $E_4$  is unstable and stable limit cycles exist. When the delay increases, the size of region  $C_\tau$  becomes larger. Furthermore, each point within  $C_\tau$  corresponds to a unique limit cycle.

For the non-delayed case  $\tau_1 = \tau_2 = 0$ , the family  $Q$  (8) (point  $F$  in Fig. 1) contains only stable equilibria, see Propositions 1 and 2. Furthermore, we will demonstrate that, under the influence of delay, some parts of the family become unstable, and the entire family may contain unstable equilibria.

Table 1 presents six points selected from the family of equilibria (8), where all three species coexist (prey–predator–superpredator). For these points,

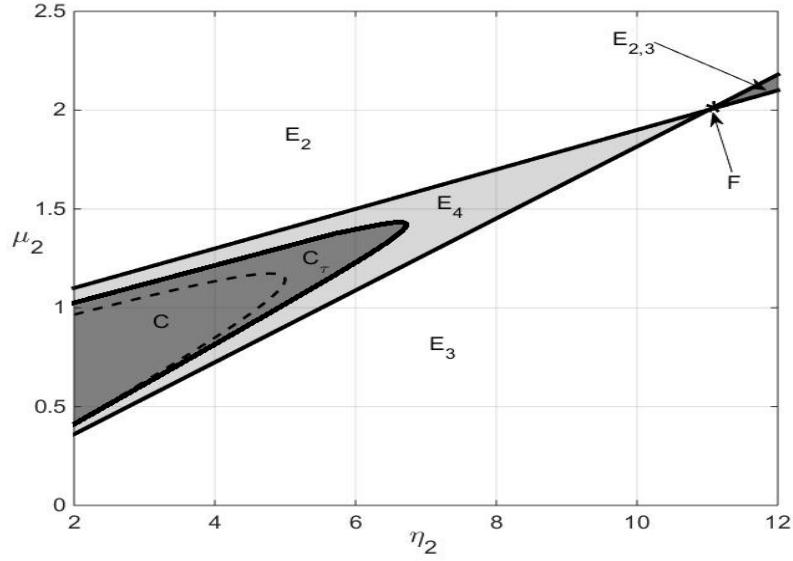


FIG. 1. Two-parameter bifurcation diagram with respect to  $\eta_2$  and  $\mu_2$ ,  $E_j$  ( $j = 2, 3, 4$ ) – regions of monostability,  $E_{2,3}$  – the region of bistability,  $C$  – the region of limit cycles without delay,  $C_\tau$  – the region of limit cycles with delay  $\tau_1 = \tau_2 = 0.05$ , point  $F$  corresponds to the family of equilibria;  $\mu_1 = 1$ ,  $\eta_1 = 10$ ,  $d_1 = 1$ ,  $d_2 = 1$ .

$i$	$Q_i(x_i, y_i, z_i)$	$\tau_2 = 0$	$\tau_2 = 0.1$	$\tau_2 = 0.3$
1	$Q_1(0.11, 0.77, 0.12)$	0.140	0.134	0.130
2	$Q_2(0.12, 0.64, 0.23)$	0.146	0.137	0.133
3	$Q_3(0.14, 0.51, 0.35)$	0.151	0.142	0.140
4	$Q_4(0.15, 0.38, 0.47)$	0.157	0.149	0.149
5	$Q_5(0.16, 0.25, 0.58)$	0.163	0.157	0.159
6	$Q_6(0.17, 0.12, 0.7)$	0.168	0.164	0.167

ТАБЛИЦА 1. Critical values  $\tau_1^{crit}$  for several equilibria from the family  $Q$  under different delay  $\tau_2$ ;  $\mu_1 = 1$ ,  $\eta_1 = 10$ ,  $d_1 = 1$ ,  $d_2 = 1$ .



we compare the bifurcation threshold  $\tau_1^{\text{crit}}$  across different delay scenarios:  $\tau_2 = 0$ ,  $\tau_2 = 0.1$  and  $\tau_2 = 0.3$ . The analysis shows that the parameter  $\tau_1^{\text{crit}}$  increases monotonically with the index  $i$  (number of an equilibrium  $Q_i$ ). Consequently, for lower values of  $i$ , where  $\tau_1$  remains below a critical threshold  $\tau_1^{\text{crit}}$ , the entire family of equilibrium points is stable. However, stability across the family  $Q$  varies with  $\tau_1^{\text{crit}}$ —while some parts remain stable, others undergo instability. These critical values determine exactly when oscillations appear in the system, illustrating how the delays  $\tau_1$  and  $\tau_2$  influence the onset of biological dynamics.

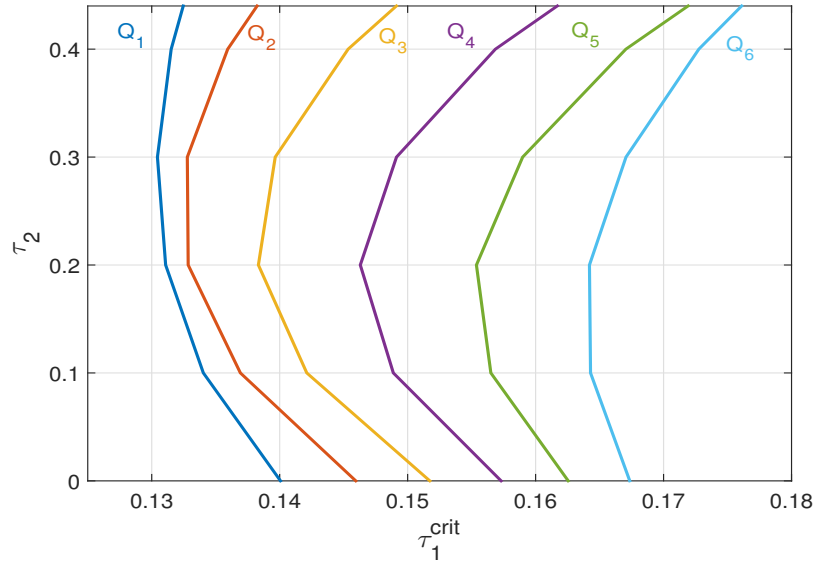


FIG. 2. Poincaré–Andronov–Hopf bifurcation curves for the family of equilibria  $Q_i$ ,  $i = 1, \dots, 6$ , in the  $(\tau_1, \tau_2)$  parameter plane;  $\mu_1 = 1$ ,  $\eta_1 = 10$ ,  $d_1 = 1$ ,  $d_2 = 1$ .

Fig. 2 presents the Poincaré–Andronov–Hopf bifurcation curves for several equilibria from the family  $Q$  (see Table 1), in the  $(\tau_1, \tau_2)$  parameter plane. Each curve delineates the boundary between the asymptotic stability of the equilibrium (to the left) and the oscillatory regime (to the right). The diagram reveals two characteristic tendencies. Firstly, for a fixed  $\tau_2$ , the critical delay  $\tau_1^{\text{crit}}$  increases monotonically with the equilibrium index  $i$ : from  $Q_1$  to  $Q_6$  the system tolerates a larger delay before losing stability. Secondly, for a fixed equilibrium  $Q_i$ , the value of  $\tau_1^{\text{crit}}$  decreases for moderate values of  $\tau_2$  and increases noticeably for larger values of  $\tau_2$ . This indicates the nonlinear dependence of  $\tau_1$  on  $\tau_2$  and the predator–prey relationship. For specific values of the delay parameters, a large superpredator-to-predator ratio ensures the stability of stationary states.

When  $\tau_1 = 0$  and  $\tau_2 \neq 0$ , the family  $Q$  (8) contains only stable equilibria. Fig. 3a shows that the trajectories converge oscillatory toward the family of equilibria (black line  $E_2E_3$ ) for different initial conditions when  $\tau_1 = 0$ ,  $\tau_2 = 1$ . For  $\tau_2 = 2$ , the trajectories exhibit faster convergence to the equilibrium family compared to  $\tau_2 = 1$  (see Fig. 3b).

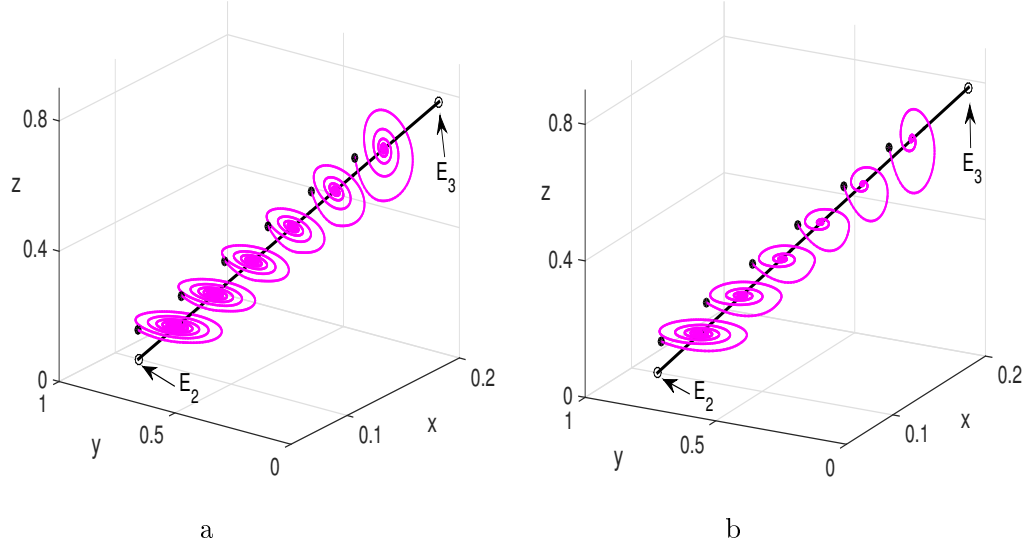


FIG. 3. Convergence to equilibria of the family  $Q$  (black line) from different initial points for  $\tau_1 = 0$ . a)  $\tau_2 = 1$ , b)  $\tau_2 = 2$ ;  $\mu_1 = 1$ ,  $\eta_1 = 10$ ,  $d_1 = 1$ ,  $d_2 = 1$ .

To illustrate the realization of stable equilibria with different initial conditions, we consider the dynamics for two sets of delays  $\tau_1$ ,  $\tau_2$ . Fig. 4 presents the basins of attraction for two representative values of the superpredator density ( $z_1 = 0.24$ ,  $z_2 = 0.57$ ). The family of equilibria  $Q$  is divided into five segments, each marked by a distinct color. Initial conditions  $(x_0, y_0)$  are colored according to the segment of  $Q$  to which the corresponding trajectory converges. One can observe a clear partition of the initial condition plane into colored sectors. The consistent ordering of colors between the family segments and the attraction sectors on the plane  $z = \text{const}$  confirms that the one-dimensional continuum of equilibria acts as a structured attractor of the delayed system.

Panel (a), corresponding to  $\tau_1 = 0.1$ ,  $\tau_2 = 0$ , shows a relatively regular partition of the phase space, where trajectories smoothly converge to different parts of the equilibrium family depending on initial conditions. In contrast, panel (b), with  $\tau_1 = 0.1$ ,  $\tau_2 = 0.2$ , demonstrates a more intricate basin geometry. The introduction of the second delay leads to a deformation of the basin boundaries, indicating an increased sensitivity to initial conditions and a more complex organization of attractors.

This figure highlights a key consequence of cosymmetry: the presence of a continuous set of equilibria gives rise to multistable behavior with distributed basins of attraction, where each equilibrium (or segment of equilibria) possesses its own domain of influence. Moreover, time delays modify not only the stability of equilibria but also the geometric structure of their basins, potentially leading to fragmentation and increased complexity in the phase space. From a biological perspective, this structure reflects the existence of multiple alternative stable configurations of the ecological system under identical environmental conditions.

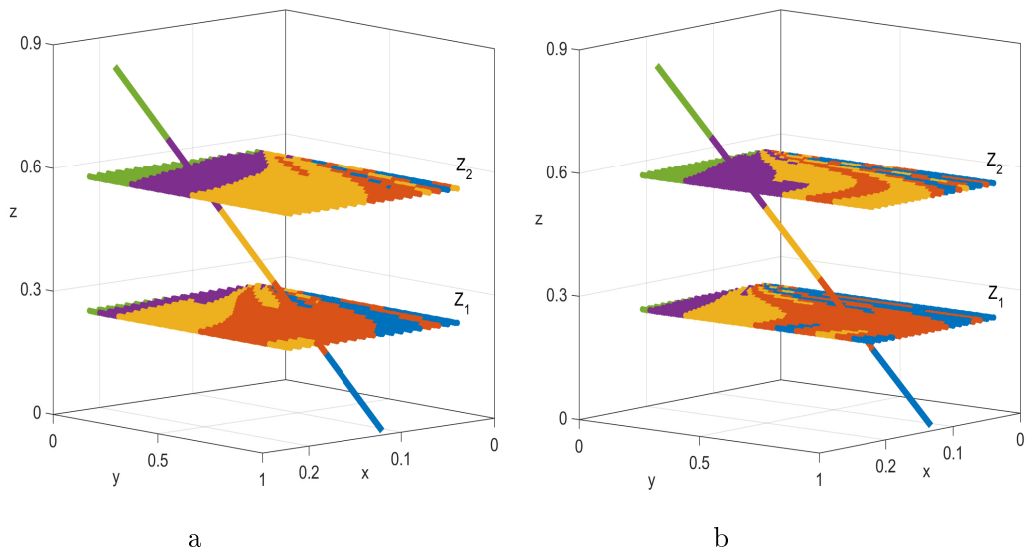


FIG. 4. Basins of attraction of system (1) for tow planes  $z = 0.24$  and  $0.57$ . The continuous family of equilibria  $Q$  is partitioned into five segments. Initial conditions  $(x_0, y_0, z_0)$  are colored according to the segment of  $Q$  to which the corresponding trajectory converges. a)  $\tau_1 = 0.1$ ,  $\tau_2 = 0$ ; b)  $\tau_1 = 0.1$ ,  $\tau_2 = 0.2$ . Other parameters are  $\mu_1 = 1$ ,  $\eta_1 = 10$ ,  $d_1 = 1$ ,  $d_2 = 1$ .

For system (1) with  $\tau_2 = 0$ ,  $\tau_1 \neq 0$  the stability of the equilibria  $Q_1$  (curve 2) and  $Q_5$  (curve 3) is analyzed using their eigenvalues (see Fig. 5). The critical bifurcation points  $\tau_1^{\text{crit}}$  are marked in red. Both  $Q_1$  (curve 2) and  $Q_5$  (curve 3) are stable for delays  $\tau_1 < \tau_1^{\text{crit}}$  and lose stability via a Poincaré–Andronov–Hopf bifurcation when  $\tau_1$  exceeds this critical value. For  $\tau_1 = \tau_1^{\text{crit}}$ , it gives a periodic solution.

For  $\tau_2 = 0$ , the Table 1 shows that the critical value  $\tau_1^{\text{crit}}$  varies from 0.14 to 0.168. So, in the case of  $\tau_1 = 0.151$ , we obtain stable and unstable equilibria, as well as a periodic solution (see Fig. 6). Fig. 6a shows the time evolution of the superpredator population for initial points from vicinity of the family

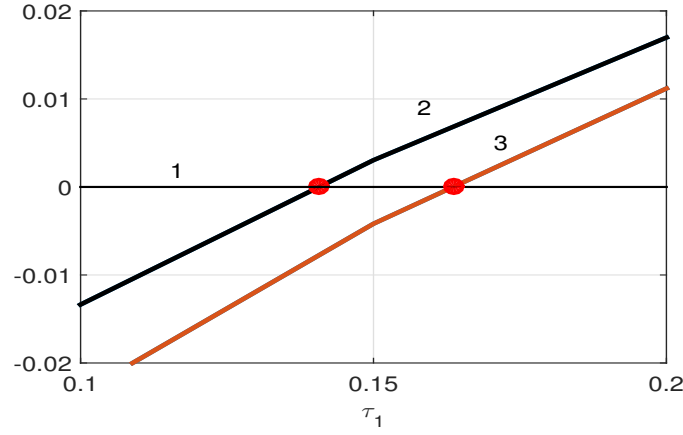


FIG. 5. Dependence upon  $\tau_1$  of real parts of the eigenvalues for Jacobian at equilibria  $Q_1$  (curves 1, 2) and  $Q_5$  (curves 1, 3),  $\tau_2 = 0$ ;  $\mu_1 = 1$ ,  $\eta_1 = 10$ ,  $d_1 = 1$ ,  $d_2 = 1$ .

of equilibria  $Q$ . The results demonstrate three distinct behaviors: a stable equilibrium at  $z = 0.7$  and  $0.58$ , an unstable equilibrium at  $z = 0.23$ , and a periodic solution  $z = 0.35$ . Fig. 6b demonstrates that trajectories converge oscillatorily towards the family of equilibria (black line  $E_2E_3$ ) when  $z = 0.7$  and  $0.58$ . A limit cycle is realized at  $z = 0.35$ , while growing oscillations at  $z = 0.23$ .

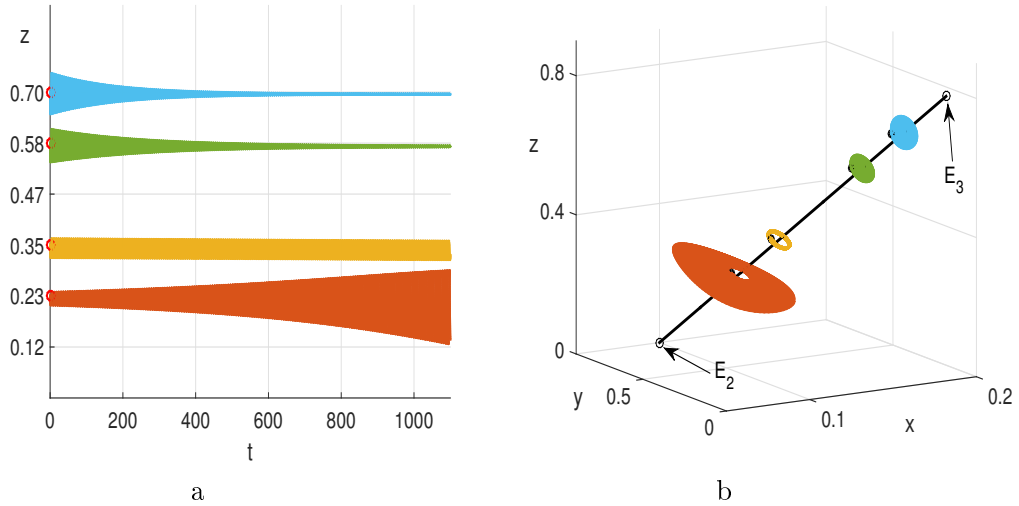


FIG. 6. Dynamics scenarios for System (1) with  $\tau_1 = 0.151$ ,  $\tau_2 = 0$ , under cosymmetry conditions (6) from different initial points;  $\mu_1 = 1$ ,  $\eta_1 = 10$ ,  $d_1 = 1$ ,  $d_2 = 1$ .

For the case  $\tau_1 = \tau_2 = \tau$ , we find that the bifurcations for the equilibria ( $Q_i, i = 1, \dots, 6$ ) occur at critical values  $\tau^{\text{crit}} = 0.133, 0.135, 0.14, 0.147, 0.155, 0.163$ , respectively. When  $\tau_1 = \tau_2 = 0.1$ , all equilibrium points  $Q_i$  are stable, see Fig. 7. The principal eigenvalues constituting the stability spectrum for these solutions  $Q_i$  have been computed and are tabulated on the right of Fig. 7.

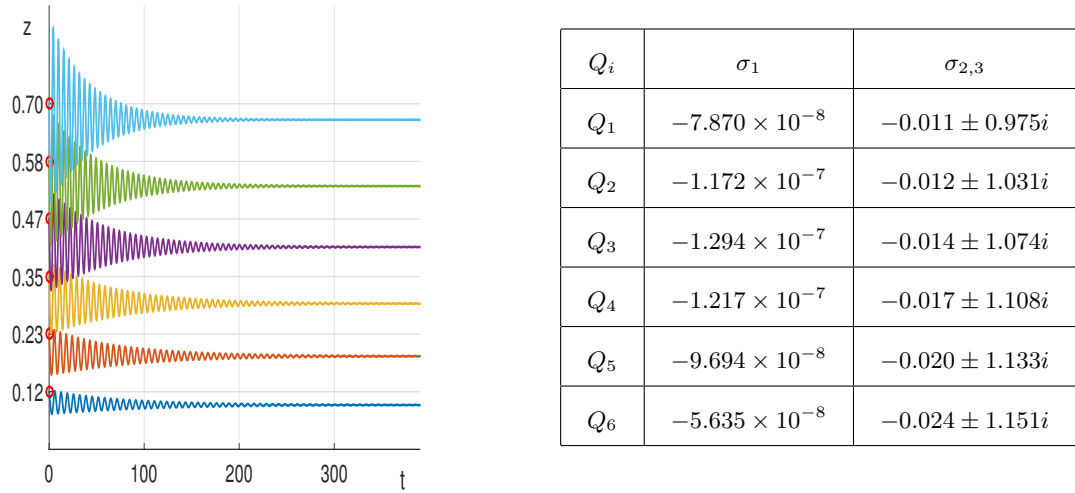


FIG. 7. Convergence to equilibria of the family  $Q$  at  $\tau_1 = \tau_2 = 0.1$  for different initial conditions (left). Main values of the stability spectrum for equilibria (right);  $\mu_1 = 1$ ,  $\eta_1 = 10$ ,  $d_1 = 1$ ,  $d_2 = 1$ .

The destabilizing effect of the delay  $\tau_1$  on the stability of family is vividly demonstrated in Fig. 8. This figure captures the phenomenon of multistability – the coexistence of multiple attractors for a single set of parameters. It is a direct consequence of cosymmetry. We fix the delay  $\tau_1 = \tau_2 = 0.14$  and select different points along the family of equilibria  $Q$  (see. Table 1). This specific value  $\tau$  is supercritical for some equilibria and subcritical for others, allowing us to observe multiple dynamical regimes simultaneously.

Fig. 8a shows the time series of the superpredator density ( $z$ ). It reveals three distinct outcomes based solely on initial conditions. At high  $z$ , the trajectories starting near the family of  $Q$  (e.g.,  $z = 0.7$  or  $0.58$ ) converge with oscillations to stable equilibria. This indicates that for these population densities, the system is resilient and returns to steady coexistence. The trajectory starting near  $z = 0.47$  evolves to a persistent, stable periodic oscillation. Here we see a Poincaré–Andronov–Hopf bifurcation, where a stable limit cycle occurs. A trajectory starting near a low-density superpredator equilibrium ( $z = 0.23$ ) deviates away from it. This indicates that this specific

equilibrium is unstable one, making coexistence at these population levels unsustainable for the given parameters.

The location of the various trajectories and objects is shown in Fig. 8b. The continuous family of equilibria  $Q$  is represented by the solid black line connecting the boundary equilibria  $E_2$  and  $E_3$ . The trajectories show how the dynamics are determined by its initial state. One can see convergence to stable equilibria on the family's line, while others are attracted to the isolated limit cycle or tend to the equilibrium  $E_2$ .

In summary, Fig. 8 provides a compelling visual representation of how the delay  $\tau$  selectively destabilizes specific segments of the continuous family of equilibria, leading to a complex landscape where stable and unstable points as well as periodic solutions coexist. This underscores the critical importance of the initial predator-superpredator proportion in the long-term scenario of delayed intraguild predation systems.

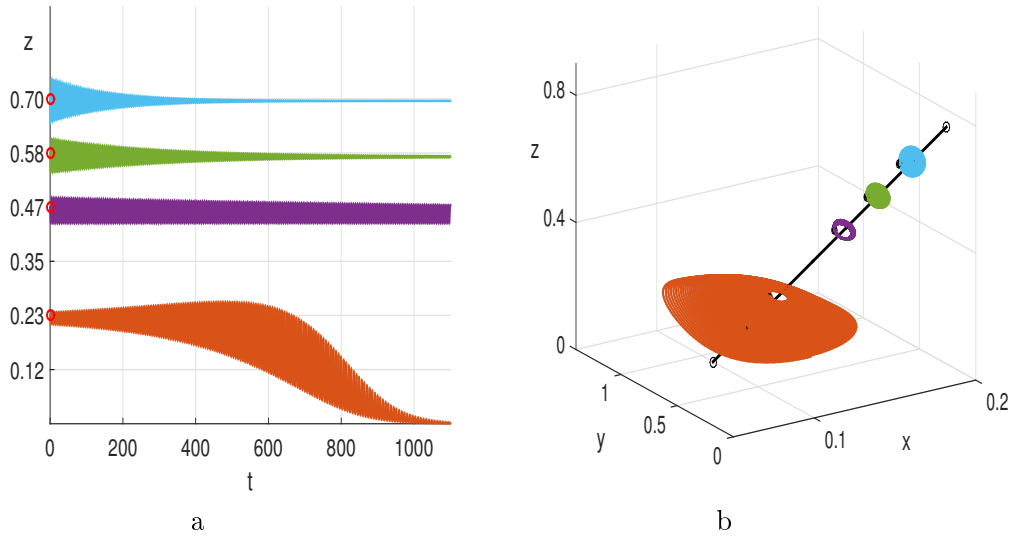


FIG. 8. Dynamics scenarios under cosymmetry conditions (6) and delay  $\tau_1 = \tau_2 = 0.14$ . Dependence of the superpredator population on time (a) and trajectories (b) originating from different initial conditions near the family of equilibria  $Q$ ;  $\mu_1 = 1$ ,  $\eta_1 = 10$ ,  $d_1 = 1$ ,  $d_2 = 1$ .

Figure 9 shows that a sufficiently large time delay can completely destabilize the entire continuous family of equilibria, leading to the emergence of persistent oscillatory dynamics. The figure 9a depicts a trajectory (shown in red), originating from an initial condition near equilibrium  $Q_6$  of the family  $Q$ . However, unlike in scenarios with smaller delays, where trajectories converge to stable equilibria of the family, this trajectory evolves into a stable limit

cycle without a superpredator. In addition to this cycle, there is also a prey–superpredator cycle (without predator), see both cycles in figure 9b.

This behavior occurs because the chosen delay  $\tau = 0.2$  exceeds the critical bifurcation value  $\tau^{\text{crit}}$  for all equilibria in the family  $Q$ . As detailed in Table. 1, the critical values for the family points  $Q_1$  to  $Q_6$  when  $\tau_1 = \tau_2$  lie in the interval  $[0.134, 0.164]$ . Since  $\tau = 0.2$  is greater than all these thresholds, every equilibrium point on the family  $Q$  has lost its stability via a Poincaré–Andronov–Hopf bifurcation. Thus, Figure 9 illustrates the powerful destabilizing role of time delays, showing that beyond a critical threshold, they can destroy the multistability in a cosymmetric system and produce oscillatory regimes in a lower-dimensional subspace.

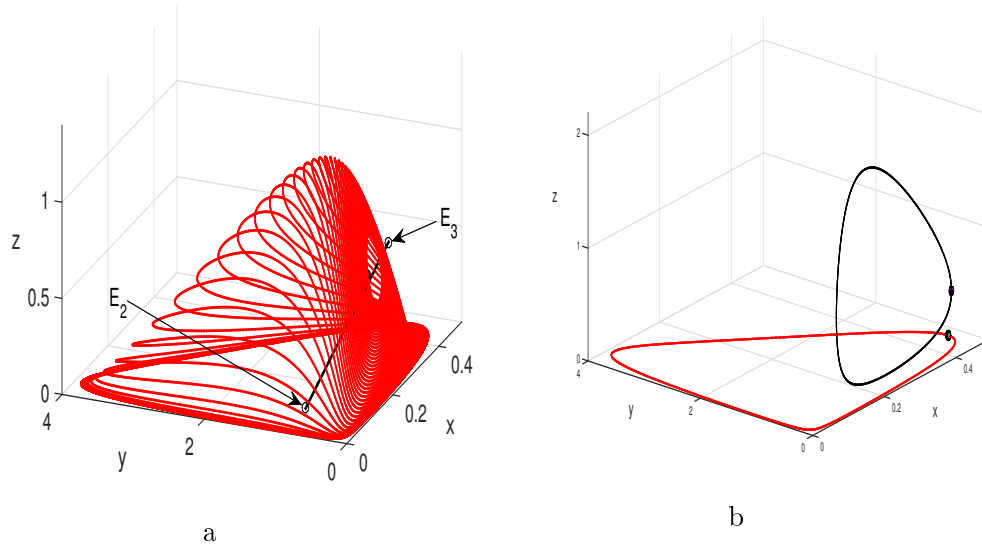


FIG. 9. Phase portrait of the system (1) for  $\tau_1 = \tau_2 = 0.2$ . a) Convergence to the limit cycle in the absence of the superpredator, b) shows the superpredator-free limit cycle (red) and the predator-free limit cycle (black), the solid black line  $E_2E_3$  represents the continuous family of equilibria  $Q$ ;  $\mu_1 = 1$ ,  $\eta_1 = 10$ ,  $d_1 = 1$ ,  $d_2 = 1$ .

## 5 Conclusions

This study presents an analytical and numerical investigation of the dynamics of a tri-trophic intraguild predation model with two distinct time delays. The main focus is on a family of equilibria that occurs in multi-species ecological models when certain additional conditions are met for parameters that characterize predator behavior. [The primary novelty of this paper, compared to previous own work on intraguild predation \(IGP\) systems \[6, 24,](#)

25], lies in its specific investigation into the combined effect of two distinct time delays on a tri-trophic model that inherently possesses a cosymmetry-induced family of equilibria.

Our results concern the role of time delays in governing the stability of the family of equilibria:

- The delay  $\tau_2$  (associated with the superpredator's handling time) is non-destabilizing; the entire family of equilibria remains stable for any  $\tau_2 > 0$  when  $\tau_1 = 0$ .
- In contrast, the delay  $\tau_1$  (associated with predator gestation) acts as a critical bifurcation parameter. The system undergoes a Poincaré–Andronov–Hopf bifurcation when  $\tau_1$  exceeds a threshold value  $\tau_1^{crit}$ , moving from stable coexistence to persistent periodic oscillations. This shows how inherent biological lags can drive population cycles in complex food webs.
- The scenario of equal delays ( $\tau_1 = \tau_2 > 0$ ) also yields a Poincaré–Andronov–Hopf bifurcation at a critical value, confirming that delays can synergistically destabilize the system.

Critical delay thresholds were calculated throughout the family of equilibria, revealing that stability does not degrade uniformly. As a result, stable and unstable equilibrium states coexist under identical parameter conditions, underscoring the system's multistable nature. Numerical simulations confirm this complex behavior, visually demonstrating trajectories that converge to stable points or form limit cycles.

Biologically, the observed multistability — where a system can sustain multiple stable states under identical environmental parameters — underscores the ecological plasticity inherent in many food webs. This phenomenon is crucial for understanding how ecosystems adapt to environmental fluctuations [31]; it reflects the concept that a community's historical trajectory can profoundly shape its future dynamics and species persistence [32]. The occurrence of stability switches, bifurcations, and oscillatory behaviours induced by time delays further elucidates irregular population fluctuations frequently observed in natural intraguild predation systems [33, 34].

To ground these findings in concrete biological scenarios, consider a well-documented terrestrial tri-trophic food web: herbivorous insects such as aphids (*Aphididae* spp.) as prey ( $x$ ), specialist predators such as ladybugs (*Coccinellidae*) as the intermediate predator ( $y$ ), and generalist insectivorous birds as the superpredator ( $z$ ), which prey on both aphids and ladybugs, thereby exhibiting intraguild predation. In this context,  $\tau_1$  corresponds to the gestation or reproductive lag of the intermediate predator (ladybugs), reflecting the time elapsed between adequate prey consumption and the recruitment of new predator offspring — a delay well documented in insect predator–prey systems [35]. The delay  $\tau_2$  represents the handling time or digestive processing delay of the superpredator (birds), a physiological constraint central to functional response models of generalist predators.



Analogous delayed dynamics arise in marine ecosystems, where zooplankton serve as prey, small planktivorous fish as intermediate predators, and larger piscivores as superpredators, with well-documented reproductive cycles and digestion-related handling times influencing population dynamics [36, 37]. Understanding these delayed interactions is essential for predicting long-term population outcomes, including species coexistence, oscillatory behaviour, and local extinction risk in response to environmental change [38, 39].

## References

- [1] A.D. Bazykin, *Nonlinear Dynamics of Interacting Populations*, World Scientific, River Edge, 1998. MR1635219
- [2] R. D. Holt, G. A. Polis, *A theoretical framework for intraguild predation*, Am. Naturalist, **149**:4 (1997), 745–764.
- [3] D. Sen, S. Ghorai, M. Banerjee, *Complex dynamics of a three species prey-predator model with intraguild predation*, Ecol. Complex, **34** (2018), 9–22.
- [4] H. Wei, *A mathematical model of intraguild predation with prey switching*, Math. Comput. Simul., **165** (2019), 107–118. Zbl 7316739
- [5] G. Ble, V. Castellanos, I.L. Hernandez, *Stable limit cycles in an intraguild predation model with general functional responses*, Math. Methods Appl. Sci., **45**:4 (2022), 2219–2233. Zbl 1533.37170
- [6] A. Almasri, V.G. Tsybulin, *A dynamic analysis of a prey-predator-superpredator system: a family of equilibria and its destruction*, Computer Research and Modeling, **15**:6 (2023), 1603–1617.
- [7] F.A. Rihan, *Delay Differential Equations and Applications to Biology*, 2nd ed., Springer, Cham, 2026.
- [8] A. Frank, S. Subbey, M. Kobras, H. Gjøsæter, *Population dynamic regulators in an empirical predator-prey system*, Journal of Theoretical Biology, **527** (2021), Article ID 110814
- [9] V.B. Kolmanovskii, A.D. Myshkis, *Introduction to the Theory and Applications of Functional Differential Equations*, Kluwer Academic Publishers, Dordrecht, 1999.
- [10] R.P. Agarwal, L. Berezhansky, E. Braverman, A. Domoshnitsky, *Nonoscillation Theory of Functional Differential Equations with Applications*, Springer, New York, 2012.
- [11] V.V. Malygina, M.V. Mulyukov, N.V. Pertsev, *On the local stability of a population dynamics model with delay*, Siberian Electronic Mathematical Reports, **11** (2014), 951–957.
- [12] K.K. Loginov, N.V. Pertsev, *Asymptotic Behavior of Solutions to a Delay Integro-Differential Equation Arising in Models of Living Systems*, Siberian Advances in Mathematics, **31**:2 (2021), 131–146.
- [13] M. A. Skvortsova, T. Yskak, *Asymptotic behavior of solutions in one predator-prey model with delay*, Siberian Math. J., **62**:2 (2021), 324–336.
- [14] F.A. Rihan, H. J. Alsakaji, C. Rajivganthi, *Stability and Hopf Bifurcation of Three-Species Prey-Predator System with Time Delays and Allee Effect*, Complexity, **2020**:1 (2020), Article ID 7306412
- [15] R. Shi, Z. Hu, *Dynamics of three-species food chain model with two delays of fear*, Chinese Journal of Physics., **77** (2022), 678–698.
- [16] W. Xu, H. Shu, L. Wang, G. Fan, *Bifurcation-Induced Species Coexistence in a Stage-Structured Intraguild Predation Model*, SIAM Journal on Applied Mathematics, **85**:2 (2025), 662–686.

- [17] S.X. Wu, X.Y. Meng, *Hopf bifurcation analysis of a multiple delays stage-structure predator-prey model with refuge and cooperation*, Electronic Research Archive, **33**:2 (2025), 995–1036.
- [18] H.J. Alsakaji, S. Kundu, F.A. Rihan, *Delay differential model of one-predator two-prey system with Monod-Haldane and holling type II functional responses*, Applied Mathematics and Computation, **397** (2021), Article ID 125919.
- [19] A. Ojha, N.K. Thakur, *Complex dynamics induced by multiple gestation delays in a Leslie-Gower-type system with competitive interference*, Mathematical Methods in the Applied Sciences, **46**:17 (2023), 17725–17759.
- [20] Y. Wang, Y. Shao, C. Chai, *Dynamics of a predator-prey model with fear effects and gestation delays*, AIMS Mathematics, **8**:3 (2023), 7535–7559.
- [21] AN. Pisarchik, U. Feudel, *Control of multistability*, Phys Rep, **540**:4 (2014), 167–218. Zbl 1357.34105
- [22] I. Bashkirtseva, AN. Pisarchik, L. Ryashko, *Multistability and stochastic dynamics of Rulkov neurons coupled via a chemical synapse*, Communications in Nonlinear Science and Numerical Simulation, **125** (2023), Article ID 107383. Zbl 1527.92014
- [23] V.N. Govorukhin, V.G. Tsybulin, *Dynamics of mechanical system with curve of equilibria: cosymmetry and multistability*, Int. J. Bifurcation and Chaos, **32**:16 (2022), Article ID 2230037.
- [24] A. Almasri, V.G. Tsybulin, *Multistability and dynamic scenarios in the prey-predator-superpredator model*, Siberian Electronic Mathematical Reports, **21**:2 (2024), 771–788.
- [25] A. Almasri, B. H. Nguyen, V.G. Tsybulin, *Continuous families of equilibria and periodic regimes in the prey-predator-superpredator system*, Vestnik Udmurtskogo Universiteta. Matematika. Mekhanika. Komp'yuternye Nauki, **35**:3 (2025), 337–355.
- [26] V.I. Yudovich, *Cosymmetry, degeneration of solutions of operator equations, and onset of a filtration convection*, Math. Notes, **49**:5 (1991), 540–545. Zbl 0747.47010
- [27] V.I. Yudovich, *Secondary cycle of equilibria in a system with cosymmetry, its creation by bifurcation and impossibility of symmetric treatment of it*, Chaos: An Interdisciplinary Journal of Nonlinear Science, **5**:2 (1995), 402–411.
- [28] V.I. Yudovich, *Bifurcations under perturbations violating cosymmetry*, Dokl. Phys., **49** (2004), 522–526.
- [29] Z. Li, B. Dai, *Global dynamics of delayed intraguild predation model with intraspecific competition*, International Journal of Biomathematics, **11**:8 (2018), Article ID 1850116.
- [30] K. Engelborghs, T. Luzyanina, D. Roose, *Numerical bifurcation analysis of delay differential equations using DDE-BIFTOOL*, ACM Transactions on Mathematical Software (TOMS), **28** (2002), 1–21.
- [31] G. Aguadé-Gorgorió, J.F. Arnoldi, M. Barbier, S. Kéfi, *A taxonomy of multiple stable states in complex ecological communities*, Ecology Letters, **27**:4 (2024), Article ID e14413.
- [32] M. Scheffer, S. Carpenter, J.A. Foley, C. Folke, B. Walker, *Catastrophic shifts in ecosystems*, Nature, **413** (2001), 591–596.
- [33] N. Sk, P.K. Tiwari, S. Pal, *A delay nonautonomous model for the impacts of fear and refuge in a three species food chain model with hunting cooperation*, Mathematics and Computers in Simulation, **192** (2022), 136–166.

- [34] B. Blasius, L. Rudolf, G. Weithoff, U. Gaedke, G.F. Fussmann, *Long-term cyclic persistence in an experimental predator-prey system*, Nature, **577** (2020), 227–230.
- [35] F. Al Basir, P.K. Tiwari, S. Samanta, *Effects of incubation and gestation periods in a prey-predator model with infection in prey*, Mathematics and Computers in Simulation, **190** (2021), 449–473.
- [36] J.H. Steele, E.W. Henderson, *The role of predation in plankton models*, Journal of Plankton Research, **14**:1 (1992), 157–172.
- [37] S.N. Raw, S.R. Sahu, *Dynamical complexities with effect of additional food and harvesting in the time delay plankton-fish model*, SeMA Journal, **81**:4 (2024), 609–640.
- [38] P. Amarasekare, *Trade-offs, temporal variation, and species coexistence in communities with intraguild predation*, Ecology, **88**:11 (2007), 2720–2728.
- [39] N.H. Fakhry, R.K. Naji, S.R. Smith?, M. Haque, *Prey fear of a specialist predator in a tri-trophic food web can eliminate the superpredator*, Frontiers in Applied Mathematics and Statistics, **8** (2022), Article ID 963991.

AHMAD ALMASRI  
SOUTHERN FEDERAL UNIVERSITY,  
MILCHAKOVA ST., 8-A,  
344006, ROSTOV ON DON, RUSSIA  
Email address: [ahmal6398@gmail.com](mailto:ahmal6398@gmail.com)

V.G. TSYBULIN  
SOUTHERN FEDERAL UNIVERSITY,  
MILCHAKOVA ST., 8-A,  
344006, ROSTOV ON DON, RUSSIA  
Email address: [vgcibulin@sfedu.ru](mailto:vgcibulin@sfedu.ru)